

Phase shifts of the light pseudoscalar meson and heavy meson scattering in heavy meson chiral perturbation theory

Bo-Lin Huang ^{*1}, Zi-Yang Lin ¹, Kan Chen¹, and Shi-Lin Zhu ^{†1}

¹*School of Physics and Center of High Energy Physics, Peking University, Beijing 100871, China*

May 6, 2022

Abstract

We calculate the complete T matrices of the elastic light pseudoscalar meson and heavy meson scattering to the third order in heavy meson chiral perturbation theory. We determine the low-energy constants by fitting to the phase shifts and scattering lengths from the lattice QCD simulations simultaneously and predict the phase shifts at the physical meson masses. The phase shifts in the $D\pi(I=1/2)$, $DK(I=0)$, $D\bar{K}(I=0)$, $D_s\bar{K}$, $D\eta$ and $D_s\eta$ S waves are so strong that bound states or resonances may be generated dynamically in all these channels. The $DK(I=0)$ channel corresponds to the well-known exotic state $D_{s0}^*(2317)$. The coupled-channel $D\pi$, $D\eta$ and $D_s\bar{K}$ scattering corresponds to the $D_0^*(2400)$. We also predict the scattering lengths and scattering volumes and observe a good convergence in the P waves and scattering volumes. Our calculations provide a possibility to accurately investigate the exotic state in the light pseudoscalar meson and heavy meson interactions.

Keywords: Chiral perturbation theory, meson-meson scattering, phase shifts

1 Introduction

The hadron-hadron interaction is one of the fundamental problems in hadronic physics. As the fundamental theory of strong interaction, quantum chromodynamics (QCD) becomes nonperturbative at low energies. Therefore, it is very difficult to use perturbative methods to derive the hadron-hadron interaction. Weinberg proposed an effective field theory (EFT) for the purpose of solving this problem in a seminal paper [1]. The EFT is formulated in terms of the most general Lagrangian consistent with the general symmetry principles, and the degrees of freedom are hadrons at low energy. The corresponding theoretical formalism is called chiral perturbation theory (ChPT) [2]. ChPT is a useful and efficient tool to study the hadronic physics at low energies [3]. However, a power-counting problem in heavy hadron ChPT occurs because of the nonvanishing heavy hadron mass in the chiral limit. The heavy baryon chiral perturbation theory (HBChPT) was proposed and developed to solve the power-counting problem which occurs in baryon ChPT [4–6]. Many achievements have been obtained in light flavor hadronic physics using SU(2) HBChPT [7–13]. Furthermore, the calculations in SU(3) HBChPT can also lead to reasonable predictions [14–21]. The infrared regularization of the covariant baryon ChPT [22] and the extended-on-mass-shell scheme [23, 24] for solving the power-counting problem are two popular relativistic approaches and have led to substantial progress in many aspects as documented in refs. [25–31]. However, HBChPT is still a well-established and versatile tool for the study of low-energy hadronic physics.

Similar to the HBChPT formalism in the light flavor meson-baryon and baryon-baryon interaction, we can use heavy meson chiral perturbation theory (HMChPT) to deal with the charmed mesons [32]. This framework can also be extended to the heavy flavor hadron interactions and the new hadron states [33–36](for a review of heavy hadron systems in ChPT, see ref. [37]).

Since the discoveries of the charm-strange meson $D_{s0}^*(2317)$ [38–40] and the hidden-charm meson $X(3872)$ [41], many investigations have been devoted to various exotic states which cannot be classified into the conventional hadrons [42–54]. The $D_{s0}^*(2317)$ inspired various explanations

*blhuang@pku.edu.cn

†zhushl@pku.edu.cn

from the different methods and pictures [55–67] (for a detailed review see ref. [68]). Some lattice QCD simulations [63, 64, 66] seemed to support the interpretation of the $D_{s0}^*(2317)$ as a DK molecule. Thus, the detailed study of the DK scattering will help us understand the nature of this exotic state. However, the light pseudoscalar meson masses are always larger than their physical masses in lattice calculations because of the shortage of the computational resources. Therefore, the extrapolation of the light pseudoscalar meson and heavy meson scattering from the nonphysical meson mass to the physical value is necessary with the help of ChPT.

In our previous papers [69, 70], we have calculated the light pseudoscalar meson and heavy meson scattering lengths up to $\mathcal{O}(p^4)$ in HMChPT. The scattering lengths were calculated through both the perturbative and iterated methods in ref. [70]. The value of the scattering length for the channel $DK(I=0)$, which involves the $D_{s0}^*(2317)$, was obtained correctly in the iterated method. In fact, the channel $DK(I=0)$ has a strong enough attractive interaction, and can lead to a negative scattering length with the iterated methods, as shown in refs. [63, 71–76]. Note that, a repulsive interaction has a negative scattering length or phase shift in our convention. The scattering length is an important observable in the scattering process, which encodes the information of the fundamental interaction. In this paper, we will calculate the complete T matrices of the elastic pseudoscalar meson and heavy meson scattering to third order in HMChPT. Then, the low-energy constants (LECs) will be determined by fitting to the phase shifts and scattering lengths simultaneously. Our study is not only concerned with the scattering lengths but also with the partial-wave phase shifts. Much more information can be obtained from the partial-wave phase shifts than the scattering lengths, because the complete information of a scattering process in the physical region is contained in partial-wave phase shifts.

This paper is organized as follows. In Sec. 2, the chiral Lagrangians are presented up to $\mathcal{O}(p^3)$. In Sec. 3, the Feynman diagrams and the results of the T matrices are presented. In Sec. 4, we outline how to derive partial-wave phase shifts and scattering lengths from the T matrices. Section 5 contains the numerical results and discussions. The last section is a brief summary.

2 Chiral Lagrangian

Our calculation of the elastic light pseudoscalar meson and heavy meson scattering is based on the effective chiral Lagrangian in HMChPT,

$$\mathcal{L}_{\text{eff}} = \mathcal{L}_{\phi\phi} + \mathcal{L}_{H\phi}. \quad (1)$$

Here, the SU(3) matrix ϕ represents the pseudoscalar Goldstone fields ($\phi = \pi, K, \bar{K}, \eta$). The lowest-order chiral Lagrangian for the Goldstone meson-meson interaction takes the form [77]

$$\mathcal{L}_{\phi\phi}^{(2)} = f^2 \text{tr}(u_\mu u^\mu + \frac{\chi_\pm}{4}). \quad (2)$$

The axial vector quantity $u^\mu = \frac{i}{2}\{\xi^\dagger, \partial^\mu \xi\}$ contains the odd number of the meson fields. The SU(3) matrix $U = \xi^2 = \exp(i\phi/f)$ collects the pseudoscalar Goldstone boson fields. The quantities $\chi_\pm = \xi^\dagger \chi \xi^\dagger \pm \xi \chi \xi$ with $\chi = \text{diag}(m_\pi^2, m_\pi^2, 2m_K^2 - m_\pi^2)$ introduce explicit chiral symmetry breaking terms. The parameter f is the pseudoscalar decay constant in the chiral limit. The lowest-order chiral Lagrangian for the heavy mesons in the heavy quark symmetry limit can be written as

$$\mathcal{L}_{H\phi}^{(1)} = -\langle (iv \cdot \partial H) \bar{H} \rangle + \langle H v \cdot \Gamma \bar{H} \rangle + g \langle H u_\mu \gamma^\mu \gamma_5 \bar{H} \rangle, \quad (3)$$

where $v_\mu = (1, 0, 0, 0)$ is the heavy meson velocity, the chiral connection $\Gamma^\mu = \frac{i}{2}[\xi^\dagger, \partial^\mu \xi]$ contains even number meson fields and the doublet of the ground state heavy mesons reads

$$H = \frac{1+\not{v}}{2}(P_\mu^* \gamma^\mu + iP\gamma_5), \quad \bar{H} = \gamma^0 H^\dagger \gamma^0 = (P_\mu^{*\dagger} \gamma^\mu + iP^\dagger \gamma_5) \frac{1+\not{v}}{2}, \quad (4)$$

$$P = (D^0, D^+, D_s^+), \quad P_\mu^* = (D^{0*}, D^{+*}, D_s^{+*})_\mu. \quad (5)$$

For the calculation of the complete T matrices up to the third order, the heavy meson Lagrangians $\mathcal{L}_{H\phi}^{(2)}$ and $\mathcal{L}_{H\phi}^{(3)}$ in the heavy quark symmetry limit read

$$\mathcal{L}_{H\phi}^{(2)} = c_0 \langle H \bar{H} \rangle \text{tr}(\chi_+) + c_1 \langle H \chi_+ \bar{H} \rangle - c_2 \langle H \bar{H} \rangle \text{tr}(v \cdot u v \cdot u) - c_3 \langle H v \cdot u v \cdot u \bar{H} \rangle$$

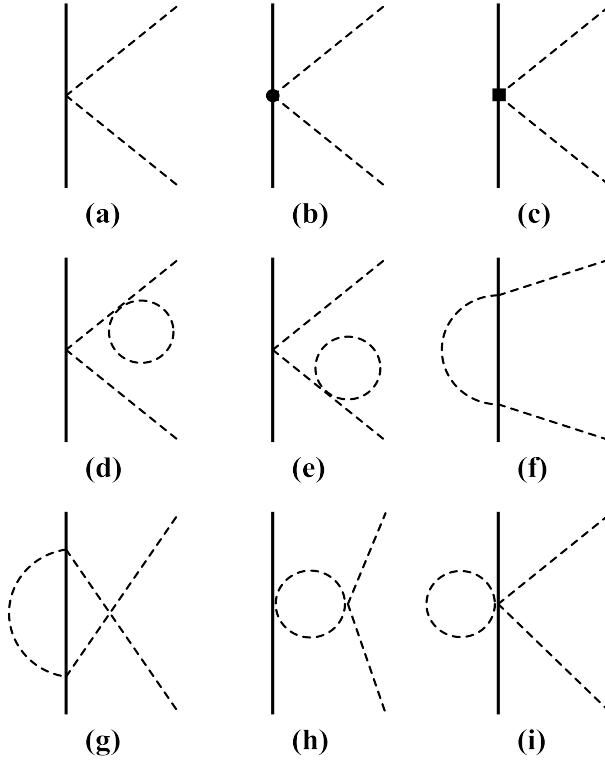


Figure 1: Tree and non-vanishing loop diagrams in the calculation of the Goldstone-heavy meson amplitudes to the third order in HMChPT. The dashed lines represent Goldstone bosons and solid lines represent pseudoscalar heavy mesons. The heavy dots and filled squares refer to the vertices from $\mathcal{L}_{H\phi}^{(2)}$ and $\mathcal{L}_{H\phi}^{(3)}$, respectively.

$$-c_4 \langle H\bar{H} \rangle \text{tr}(u^\mu u_\mu) - c_5 \langle H u^\mu u_\mu \bar{H} \rangle, \quad (6)$$

$$\mathcal{L}_{H\phi}^{(3)} = \kappa_1 \langle H[\chi_-, v \cdot u]\bar{H} \rangle + i\kappa_2 \langle H[v \cdot u, [v \cdot \partial, v \cdot u]]\bar{H} \rangle + i\kappa_3 \langle H[u^\mu, [v \cdot \partial, u_\mu]]\bar{H} \rangle. \quad (7)$$

3 T matrices

In this work, we are considering only the elastic light pseudoscalar meson and heavy meson scattering processes $M(\mathbf{q}) + H(-\mathbf{q}) \rightarrow M(\mathbf{q}') + H(-\mathbf{q}')$ in the center-of-mass frame with $|\mathbf{q}| = |\mathbf{q}'| = q$. The leading order (LO) amplitudes resulting from diagram (a) in Fig. 1 read

$$\begin{aligned} T_{\pi D}^{(1/2, \text{LO})} &= \frac{2w_\pi}{f_\pi^2}, & T_{\pi D}^{(3/2, \text{LO})} &= -\frac{w_\pi}{f_\pi^2}, & T_{\pi D_s}^{(\text{LO})} &= 0, & T_{KD}^{(1, \text{LO})} &= 0, & T_{KD}^{(0, \text{LO})} &= \frac{2w_K}{f_K^2}, \\ T_{KD_s}^{(\text{LO})} &= -\frac{w_K}{f_K^2}, & T_{\bar{K}D}^{(1, \text{LO})} &= -\frac{w_K}{f_K^2}, & T_{\bar{K}D}^{(0, \text{LO})} &= \frac{w_K}{f_K^2}, & T_{\bar{K}D_s}^{(\text{LO})} &= \frac{w_K}{f_K^2}, & T_{\eta D}^{(\text{LO})} &= 0, & T_{\eta D_s}^{(\text{LO})} &= 0, \end{aligned} \quad (8)$$

where $K = (K^+, K^0)^T$, $\bar{K} = (\bar{K}^0, K^-)^T$. The first superscripts of the T matrices denote the total isospin. In the channels with an isoscalar η -meson or D_s -meson, the total isospin is unique and does not need to be specified. The quantities $w_\phi = (m_\phi^2 + q^2)^{1/2}$ with $\phi = (\pi, K, \eta)$ denote the center-of-mass energy of the light pseudoscalar mesons. We take the renormalized (non-zero quark mass) decay constants f_ϕ instead of f (zero quark mass, the chiral limit value).

At the next-to-leading order (NLO), one has the contributions from the diagram (b) of Fig. 1, which involves the vertex from the Lagrangian $\mathcal{L}_{H\phi}^{(2)}$. The amplitudes involving the low-energy constants (LECs) read

$$T_{\pi D}^{(1/2, \text{NLO})} = \frac{1}{f_\pi^2} [8c_0 m_\pi^2 - 4c_1 m_\pi^2 + 2c_2 w_\pi^2 + c_3 w_\pi^2 + 2c_4 (w_\pi^2 - q^2 z) + c_5 (w_\pi^2 - q^2 z)], \quad (9)$$

$$T_{\pi D}^{(3/2, \text{NLO})} = \frac{1}{f_\pi^2} [8c_0 m_\pi^2 - 4c_1 m_\pi^2 + 2c_2 w_\pi^2 + c_3 w_\pi^2 + 2c_4 (w_\pi^2 - q^2 z) + c_5 (w_\pi^2 - q^2 z)], \quad (10)$$

$$T_{\pi D_s}^{(\text{NLO})} = \frac{1}{f_\pi^2} [8c_0 m_\pi^2 + 2c_2 w_\pi^2 + 2c_4 (w_\pi^2 - q^2 z)], \quad (11)$$

$$T_{KD}^{(1, \text{NLO})} = \frac{1}{f_K^2} [8c_0 m_K^2 + 2c_2 w_K^2 + 2c_4 (w_K^2 - q^2 z)], \quad (12)$$

$$T_{KD}^{(0, \text{NLO})} = \frac{1}{f_K^2} [8c_0 m_K^2 - 8c_1 m_K^2 + 2c_2 w_K^2 + 2c_3 w_K^2 + 2c_4 (w_K^2 - q^2 z) + 2c_5 (w_K^2 - q^2 z)], \quad (13)$$

$$T_{KD_s}^{(\text{NLO})} = \frac{1}{f_K^2} [8c_0 m_K^2 - 4c_1 m_K^2 + 2c_2 w_K^2 + c_3 w_K^2 + 2c_4 (w_K^2 - q^2 z) + c_5 (w_K^2 - q^2 z)], \quad (14)$$

$$T_{\bar{K}D}^{(1, \text{NLO})} = \frac{1}{f_K^2} [8c_0 m_K^2 - 4c_1 m_K^2 + 2c_2 w_K^2 + c_3 w_K^2 + 2c_4 (w_K^2 - q^2 z) + c_5 (w_K^2 - q^2 z)], \quad (15)$$

$$T_{\bar{K}D}^{(0, \text{NLO})} = \frac{1}{f_K^2} [8c_0 m_K^2 + 4c_1 m_K^2 + 2c_2 w_K^2 - c_3 w_K^2 + 2c_4 (w_K^2 - q^2 z) - c_5 (w_K^2 - q^2 z)], \quad (16)$$

$$T_{\bar{K}D_s}^{(\text{NLO})} = \frac{1}{f_K^2} [8c_0 m_K^2 - 4c_1 m_K^2 + 2c_2 w_K^2 + c_3 w_K^2 + 2c_4 (w_K^2 - q^2 z) + c_5 (w_K^2 - q^2 z)], \quad (17)$$

$$T_{\eta D}^{(\text{NLO})} = \frac{1}{3f_\eta^2} [24c_0 m_\eta^2 - 4c_1 m_\pi^2 + 6c_2 w_\eta^2 + c_3 w_\eta^2 + 6c_4 (w_\eta^2 - q^2 z) + c_5 (w_\eta^2 - q^2 z)], \quad (18)$$

$$T_{\eta D_s}^{(\text{NLO})} = \frac{1}{3f_\eta^2} [24c_0 m_\eta^2 - 16c_1 (2m_K^2 - m_\pi^2) + 6c_2 w_\eta^2 + 4c_3 w_\eta^2 + 6c_4 (w_\eta^2 - q^2 z) + 4c_5 (w_\eta^2 - q^2 z)], \quad (19)$$

where $z = \cos \theta$ is the cosine of the angle θ between \mathbf{q} and \mathbf{q}' .

At the next-to-next-to-leading order (N2LO), one has contributions from diagram (c) in Fig. 1, which involves the vertex from the Lagrangian $\mathcal{L}_{H\phi}^{(3)}$. The amplitudes read

$$T_{\pi D}^{(1/2, \text{N2LO})} = \frac{1}{f_\pi^2} [16\bar{\kappa}_1 m_\pi^2 w_\pi + 4\bar{\kappa}_2 w_\pi^3 + 4\bar{\kappa}_3 w_\pi (w_\pi^2 - q^2 z)], \quad (20)$$

$$T_{\pi D}^{(3/2, \text{N2LO})} = \frac{1}{f_\pi^2} [-8\bar{\kappa}_1 m_\pi^2 w_\pi - 2\bar{\kappa}_2 w_\pi^3 - 2\bar{\kappa}_3 w_\pi (w_\pi^2 - q^2 z)], \quad (21)$$

$$T_{\pi D_s}^{(\text{N2LO})} = 0, \quad (22)$$

$$T_{KD}^{(1, \text{N2LO})} = 0, \quad (23)$$

$$T_{KD}^{(0, \text{N2LO})} = \frac{1}{f_K^2} [16\bar{\kappa}_1 m_K^2 w_K + 4\bar{\kappa}_2 w_K^3 + 4\bar{\kappa}_3 w_K (w_K^2 - q^2 z)], \quad (24)$$

$$T_{KD_s}^{(\text{N2LO})} = \frac{1}{f_K^2} [-8\bar{\kappa}_1 m_K^2 w_K - 2\bar{\kappa}_2 w_K^3 - \bar{\kappa}_3 (w_K^2 - q^2 z)], \quad (25)$$

$$T_{\bar{K}D}^{(1,N2LO)} = \frac{1}{f_K^2} [-8\bar{\kappa}_1 m_K^2 w_K - 2\bar{\kappa}_2 w_K^3 - \bar{\kappa}_3 (w_K^2 - q^2 z)], \quad (26)$$

$$T_{\bar{K}D}^{(0,N2LO)} = \frac{1}{f_K^2} [8\bar{\kappa}_1 m_K^2 w_K + 2\bar{\kappa}_2 w_K^3 + \bar{\kappa}_3 (w_K^2 - q^2 z)], \quad (27)$$

$$T_{\bar{K}D_s}^{(N2LO)} = \frac{1}{f_K^2} [8\bar{\kappa}_1 m_K^2 w_K + 2\bar{\kappa}_2 w_K^3 + \bar{\kappa}_3 (w_K^2 - q^2 z)], \quad (28)$$

$$T_{\eta D}^{(N2LO)} = 0, \quad (29)$$

$$T_{\eta D_s}^{(N2LO)} = 0. \quad (30)$$

At this order, one also has the amplitudes from the one-loop diagrams. The nonvanishing one-loop diagrams generated by the vertices of $\mathcal{L}_{\phi\phi}^{(2)}$ and $\mathcal{L}_{H\phi}^{(1)}$ are shown in the second and third row of Fig. 1. Note that, the third-order scale-independent LECs $\bar{\kappa}_1$, $\bar{\kappa}_2$ and $\bar{\kappa}_3$ are used in the counterterm T matrices, as done in ref. [9]. Putting all amplitudes from different one-loop diagrams together, we have

$$T_{\pi D}^{(1/2,LOOP)} = -\frac{w_\pi}{12f_\pi^4} \{3w_\pi [3J_0(-w_\pi, m_K) + 4J_0(-w_\pi, m_\pi) - 9J_0(w_\pi, m_K) - 17J_0(w_\pi, m_\pi)] \\ + 12I_2(t, m_K) + 16I_2(t, m_\pi)\}, \quad (31)$$

$$T_{\pi D}^{(3/2,LOOP)} = \frac{w_\pi}{6f_\pi^4} \{3w_\pi [3J_0(-w_\pi, m_K) + 7J_0(-w_\pi, m_\pi) + J_0(w_\pi, m_\pi)] + 3I_2(t, m_K) \\ + 4I_2(t, m_\pi)\}, \quad (32)$$

$$T_{\pi D_s}^{(LOOP)} = \frac{w_\pi^2}{2f_\pi^4} [J_0(w_\pi, m_K) + J_0(-w_\pi, m_K)], \quad (33)$$

$$T_{\bar{K}D}^{(1,LOOP)} = \frac{w_K}{2f_K^4} \{w_K [J_0(-w_K, m_K) + J_0(w_K, m_\pi)] + 2I_2(t, m_\pi) - I_2(t, m_K)\}, \quad (34)$$

$$T_{\bar{K}D}^{(0,LOOP)} = \frac{w_K}{12f_K^4} \{3w_K [2J_0(-w_K, m_K) + 24J_0(w_K, m_\eta) + 22J_0(w_K, m_K) + J_0(w_K, m_\pi)] \\ - 10I_2(t, m_K) - 36I_2(t, m_\pi)\}, \quad (35)$$

$$T_{\bar{K}D_s}^{(LOOP)} = \frac{w_K}{12f_K^4} \{3w_K [12J_0(-w_K, m_\eta) + 7J_0(-w_K, m_K) + 5J_0(-w_K, m_\pi) + 2J_0(w_K, m_K)] \\ + 14I_2(t, m_K)\}, \quad (36)$$

$$T_{\bar{K}D}^{(1,LOOP)} = \frac{w_K}{24f_K^4} \{3w_K [24J_0(-w_K, m_\eta) + 22J_0(-w_K, m_K) + 3J_0(-w_K, m_\pi) + 4J_0(w_K, m_K)] \\ + 16I_2(t, m_K) + 24I_2(t, m_\pi)\}, \quad (37)$$

$$T_{\bar{K}D}^{(0,LOOP)} = \frac{w_K}{24f_K^4} \{3w_K [-24J_0(-w_K, m_\eta) - 22J_0(-w_K, m_K) + 5J_0(-w_K, m_\pi) + 4J_0(w_K, m_K)] \\ + 8I_2(t, m_K) - 72I_2(t, m_\pi)\}, \quad (38)$$

$$T_{\bar{K}D_s}^{(LOOP)} = \frac{w_K}{12f_K^4} \{3w_K [2J_0(-w_K, m_K) + 12J_0(w_K, m_\eta) + 7J_0(w_K, m_K) + 5J_0(w_K, m_\pi)] \\ - 14I_2(t, m_K)\}, \quad (39)$$

$$T_{\eta D}^{(\text{LOOP})} = \frac{3w_\eta^2}{4f_\eta^4} [J_0(-w_\eta, m_K) + J_0(w_\eta, m_K)], \quad (40)$$

$$T_{\eta D_s}^{(\text{LOOP})} = \frac{21w_\eta^2}{8f_\eta^4} [J_0(-w_\eta, m_K) + J_0(w_\eta, m_K)], \quad (41)$$

where

$$J_0(w, m) = \frac{w}{8\pi^2} + \begin{cases} \frac{1}{4\pi^2} \sqrt{w^2 - m^2} \ln \frac{-w + \sqrt{w^2 - m^2}}{m} & (w < -m), \\ -\frac{1}{4\pi^2} \sqrt{m^2 - w^2} \arccos \frac{-w}{m} & (-m < w < m), \\ \frac{1}{4\pi^2} \sqrt{w^2 - m^2} \left(i\pi - \ln \frac{w + \sqrt{w^2 - m^2}}{m} \right) & (w > m), \end{cases} \quad (42)$$

$$I_2(t, m) = \frac{1}{48\pi^2} \left\{ 2m^2 - \frac{5t}{12} - \frac{(4m^2 - t)^{3/2}}{2\sqrt{-t}} \ln \frac{\sqrt{4m^2 - t} + \sqrt{-t}}{2m} \right\}, \quad (43)$$

with $t = 2q^2(z - 1)$.

4 Partial-wave phase shifts and scattering lengths

The partial-wave amplitudes $f_l^{(I)}(q)$, where l refers to the orbital angular momentum, are obtained from the T matrix by a projection:

$$f_l^{(I)}(q) = \frac{M_H}{8\pi\sqrt{s}} \int_{-1}^{+1} dz [T_{\phi H}^{(I)} P_l(z)], \quad (44)$$

where $P_l(z)$ denotes the conventional Legendre polynomial, and $\sqrt{s} = (m_\phi^2 + q^2)^{1/2} + (M_H^2 + q^2)^{1/2}$ is the total center-of-mass energy. For the channels which may generate the bound states or resonances, the T matrix must be iterated to the infinite order. We only consider the T matrix up to the third order in the calculation of the phase shifts and scattering lengths. Therefore, we do not aim to achieve the description of the bound states or resonances. For the energy range considered in this paper, the phase shifts without the effect of the bound states or resonances $\delta_l^{(I)}(q)$ are calculated by (also see refs. [9, 78])

$$\delta_l^{(I)}(q) = \arctan[q \text{Re} f_l^{(I)}(q)]. \quad (45)$$

Based on relativistic kinematics, there is the relation between the center-of-mass momentum and the momentum of the incident light pseudoscalar meson in the laboratory system,

$$q^2 = \frac{M_H^2 p_{\text{lab}}^2}{m_\phi^2 + M_H^2 + 2M_H \sqrt{m_\phi^2 + p_{\text{lab}}^2}}. \quad (46)$$

The scattering lengths for the S waves and the scattering volumes for P waves are obtained by dividing out the threshold behavior of the respective partial-wave amplitude and approaching the threshold [79]

$$a_l^{(I)} = \lim_{q \rightarrow 0} q^{-2l} f_l^{(I)}(q). \quad (47)$$

5 Results and discussion

In order to determine the low-energy constants, we start by fitting both phase shifts and scattering lengths from the lattice QCD simulations at the nonphysical meson values simultaneously, and then make predictions for the phase shifts and the threshold parameters in all channels at the physical meson values.

Table 1: Results of fitting to various lattice data of the phase shifts and scattering lengths. For a detailed description, see the main text.

	Values	c_0	c_1	c_2	c_3	c_4	c_5	$\bar{\kappa}_1$	$\bar{\kappa}_2$	$\bar{\kappa}_3$
c_0 (GeV $^{-1}$)	-0.77 ± 0.39	1.00	0.99	-0.86	-0.88	0.00	0.00	0.02	-0.92	0.00
c_1 (GeV $^{-1}$)	-0.64 ± 0.35		1.00	-0.86	-0.89	0.00	0.00	0.01	-0.93	0.00
c_2 (GeV $^{-1}$)	-5.04 ± 1.83			1.00	0.95	-0.51	-0.41	-0.01	0.61	0.50
c_3 (GeV $^{-1}$)	5.47 ± 1.57				1.00	-0.36	-0.45	0.10	0.67	0.40
c_4 (GeV $^{-1}$)	8.99 ± 0.93					1.00	0.80	0.00	0.37	-0.98
c_5 (GeV $^{-1}$)	-3.08 ± 0.70						1.00	0.00	0.34	-0.90
$\bar{\kappa}_1$ (GeV $^{-2}$)	0.21 ± 0.04							1.00	0.01	0.00
$\bar{\kappa}_2$ (GeV $^{-2}$)	7.81 ± 3.88								1.00	-0.38
$\bar{\kappa}_3$ (GeV $^{-2}$)	-1.87 ± 1.47									1.00
$\chi^2/\text{d.o.f.}$	$\frac{34.85}{195-9} = 0.19$									

5.1 Fitting

Now we determine $c_{0,\dots,5}$ and $\bar{\kappa}_{1,2,3}$ using the phase shifts and the scattering lengths from lattice data. We take the S -wave phase shifts with $I = 3/2$ and the P -wave phase shifts with $I = 1/2$ of the elastic $D\pi$ scattering at $m_\pi \simeq 391$ MeV from ref. [80]. The S -wave phase shift with $I = 1/2$ of the $D\pi$ scattering is not used in the fitting because there exists a near-threshold bound state which cannot be obtained in the perturbative method. The P -wave phase shift with $I = 0$ of the elastic DK scattering at $m_\pi \simeq 239$ MeV is taken from ref. [66]. Again, there exists a bound state, i.e., $D_{s0}^*(2317)$, in the S -wave $I = 0$ DK channel, and then the phase shift from this channel is not used to determine the LECs. The phase shifts of the elastic $D\bar{K}$ scattering are obtained by using a simple parametrization with the scattering lengths in ref. [66]. Therefore, we use the $D\bar{K}$ scattering lengths directly, instead of the phase shifts. For the three phase shifts which are used to determine the LECs, we take the data with the pion (kaon) lab-momentum between 5 and 300 MeV. In addition, the scattering lengths of the five channels [$D\bar{K}(I = 0)$, $D\bar{K}(I = 1)$, $D\pi(I = 3/2)$, $D_s K$, $D_s \pi$] are used to determine the LECs from refs. [63, 66, 80]. We take the scattering length of the channel [$D\pi(I = 3/2)$] at $m_\pi \simeq 391$ MeV from ref. [80], the scattering lengths of the channels [$D\bar{K}(I = 0)$, $D\bar{K}(I = 1)$] at $m_\pi = 239$ MeV and $m_\pi = 391$ MeV from ref. [66], and the (M007, M010) data for the five channels from ref. [63]. The corresponding lattice values of f_π and f_K are from ref. [81], and we always choose $f_\eta = 1.2f_\pi$ in this paper. The resulting LECs with the correlations between the parameters can be found in Table 1. The uncertainty for the respective parameter is statistical, and it measures how much a particular parameter can be changed while maintaining a good description of the fitting data. Nevertheless, the parameters cannot really vary independently of each other because of the mutual correlations, as detailed in refs. [82, 83]. Therefore, the large uncertainties of some LECs in our fit cannot make the errors of the phase shifts and the threshold parameters become large, because a full error analysis requires a complete covariance matrix. However, we obtain a small uncertainties for some LECs (e.g. c_4 , c_5 , $\bar{\kappa}_1$). Furthermore, the values of the LECs are of natural size. The absolute value of the correlation between c_0 and c_1 is very close to one, which is consistent with the fact that the terms with these two parameters only involve the masses of the light pseudoscalar mesons.

The corresponding phase shifts and scattering lengths from the fitting are shown in Fig. 2. The S -wave phase shifts with $I = 3/2$ and P -wave phase shifts with $I = 1/2$ of the $D\pi$ scattering at $m_\pi \simeq 391$ MeV are in very good agreement with the data from lattice QCD simulations up to the pion lab-momentum 300 MeV. For the isoscalar P -wave DK scattering at $m_\pi \simeq 239$ MeV, the values of the phase shifts are very consistent with the data from lattice QCD simulations below the kaon lab-momentum 200 MeV. However, the P -wave phase shifts of the $DK(I = 0)$ from lattice QCD simulations have large errors. The values of the $DK(I = 0)$ P -wave phase shifts are in agreement with the results from lattice QCD within errors up to the kaon lab-momentum 300 MeV. The scattering length of the $D\pi(I = 3/2)$ at $m_\pi \simeq 391$ MeV is in agreement with the value of the lattice QCD from ref. [80] within errors. The scattering lengths of the $D\bar{K}(I = 1)$ at $m_\pi = 239, 391$ MeV and the $D\bar{K}(I = 0)$ at $m_\pi = 391$ MeV are in good agreement with the

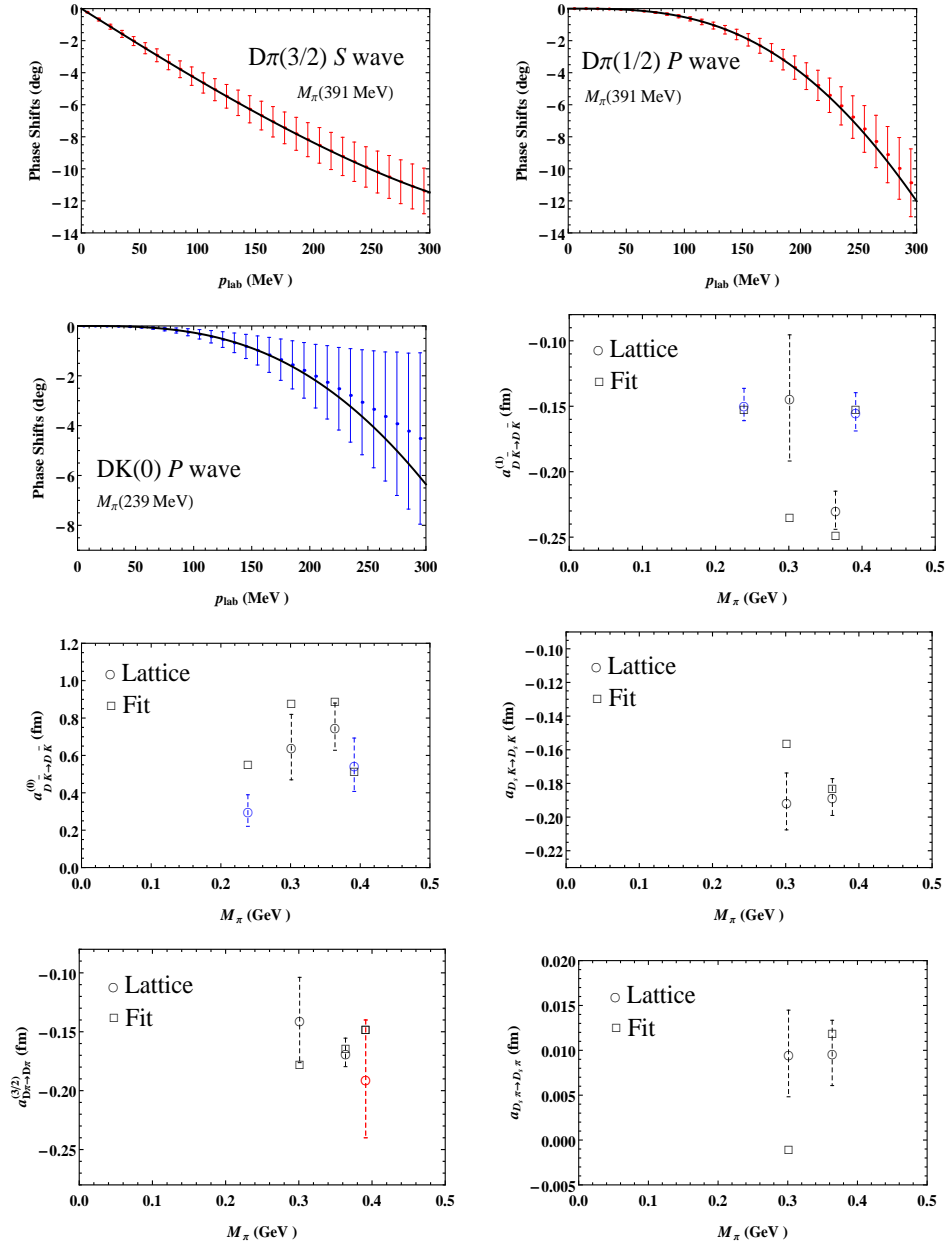


Figure 2: Fits for the light pseudoscalar meson and D meson phase shifts and scattering lengths from various lattice data. The lattice phase shifts and scattering length with the red error bars in the $D\pi(I = 3/2)$ S -wave, $D\pi(I = 1/2)$ P -wave and $a_{D\pi \rightarrow D\pi}^{(3/2)}$ are from ref. [80]. The lattice data with the blue error bars in the $DK(I = 0)$ P -wave, $a_{D\bar{K} \rightarrow D\bar{K}}^{(1)}$ and $a_{D\bar{K} \rightarrow D\bar{K}}^{(0)}$ are from ref. [66]. The lattice scattering lengths with the black error bars are from ref. [63]. For a detailed description of the fits, see the main text.

values of the lattice QCD from ref. [66]. The value for the $D\bar{K}(I = 0)$ at $m_\pi = 239$ MeV has a small deviation from the lattice QCD. The reason is that there may exist a virtual bound state in this channel. The scattering lengths of the five channels [$D\bar{K}(I = 0)$, $D\bar{K}(I = 1)$, $D\pi(I = 3/2)$, $D_s K$, $D_s \pi$] at $m_\pi \simeq 301, 364$ MeV are in agreement with the values of the lattice QCD from ref. [63] within errors. There exist small deviations in a few points because the values of the lattice QCD are from different groups, which may cause some errors in this fitting. However, to sum up, we obtain a good description of the three phase shifts and the five scattering lengths at the nonphysical meson values.

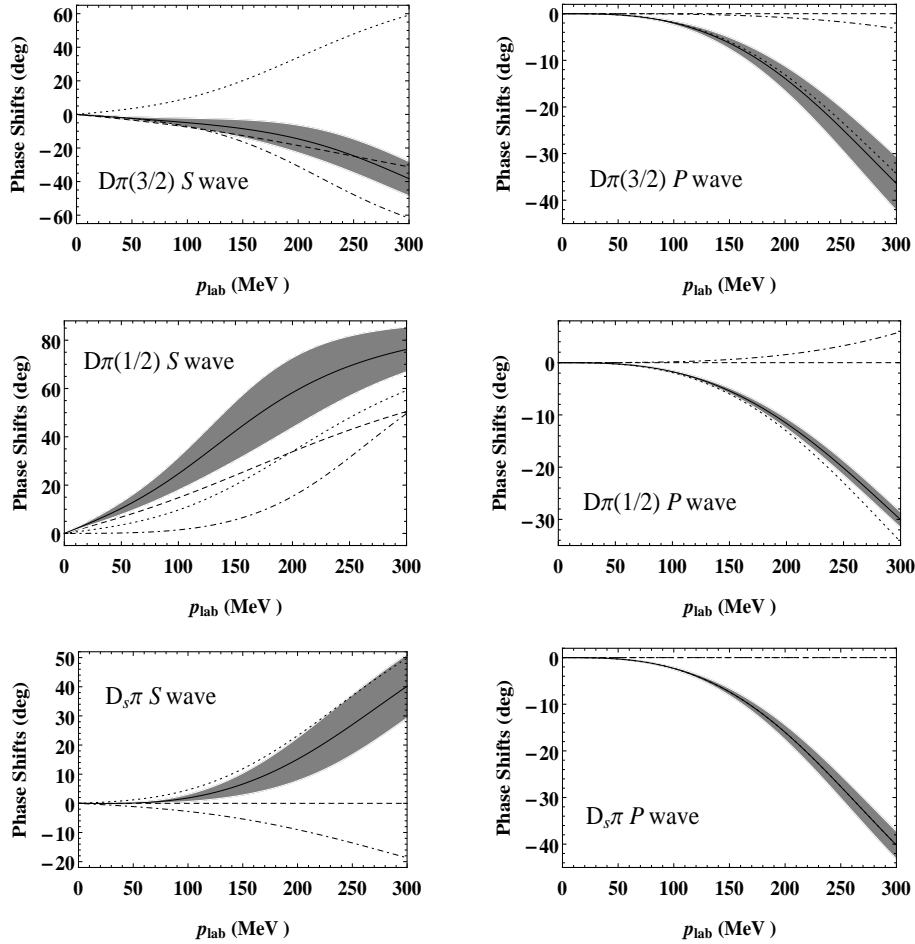


Figure 3: Predictions for the pion- D meson phase shifts versus the pion laboratory momentum at physical meson values. The dashed, dotted, dash-dotted and solid lines denote the first-, second-, third-order and their total contributions, respectively. The error bands are estimated from the statistical errors of the LECs using the standard error propagation formula with the correlations.

5.2 Phase shifts

In the following, we make predictions of the S - and P -wave phase shifts for the eleven channels at the physical meson values using the LECs determined above. We use the values of the physical parameters: $m_\pi = 139.57$ MeV, $m_K = 493.68$ MeV, $f_\pi = 92.07$ MeV, $f_K = 110.03$ MeV, $M_D = 1869.66$ MeV, $M_{D_s} = 1968.35$ MeV from PDG [84]. The numerical results of the phase shifts of the pion-, kaon-, antikaon-, and eta- D meson scatterings are shown in Figs. 3-6, respectively. The error bands of the phase shifts in the total contributions are estimated from the statistical errors of the LECs using the standard error propagation formula with the correlations. We can see that the bands from the LECs are not too large to be unacceptable. The bands in the different orders are not given because we do not determine the LECs at the corresponding orders, although we present the values of the phase shifts from the different orders. The convergence is not good for most of the S -wave phase shifts, which is not surprising because it is difficult to achieve a good convergence at the third chiral order, as in the case of the pion-nucleon scattering [9]. However, the P -wave phase shifts at the third chiral order are much smaller than those at the second chiral order, which indicates a good convergence.

For the pion- D meson phase shifts, we obtain the repulsions in the $D\pi(I = 3/2)$ S wave and all P waves, and attractions in the $D\pi(I = 1/2)$ and $D_s\pi$ S waves. It is clear that there exist no bound states or resonances in the channels with repulsions. The attraction is weak below 200 MeV in the $D_s\pi$ S wave. It should not be strong enough to generate a bound state or resonance in this wave. The $D\pi(I = 1/2)$ S wave is particularly interesting. The attraction exists at each order, and the total attraction is very strong even below 200 MeV. The results from lattice QCD simulations at the nonphysical meson values support that there exists a bound state

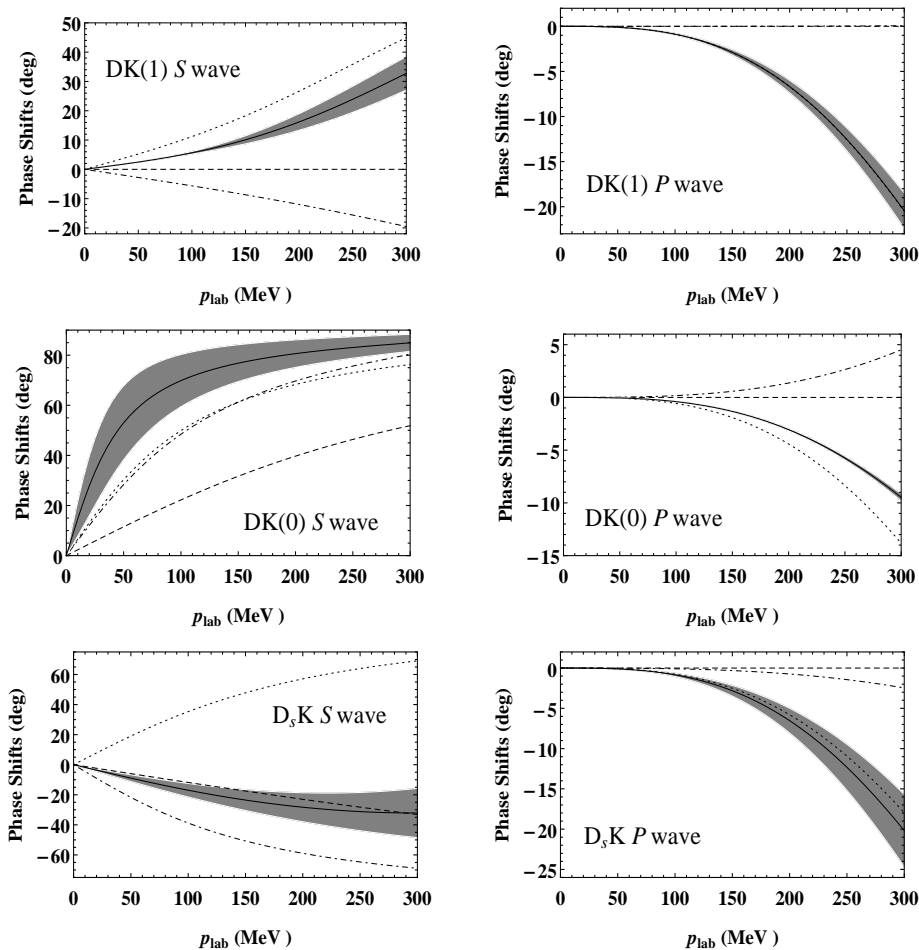


Figure 4: Predictions for the kaon- D meson phase shifts versus the kaon laboratory momentum at physical meson values. The notation is the same as in Fig. 3.

or resonance in this channel [80, 85]. However, the production of a bound state or resonance requires the nonperturbative dynamics through an iterated method. The calculations including the nonperturbative dynamics will be presented in the forthcoming works.

For the kaon- D meson phase shifts, there are repulsions in the $D_s K$ S wave and all P waves, and then the bound state or resonance cannot be dynamically generated in these waves. The $DK(I=1)$ S wave has weak attractions which cannot generate a bound state or resonance. As expected, we obtain a strong attraction in the $DK(I=0)$ S wave. This wave corresponds to the well-known bound state $D_{s0}^*(2317)$. But this exotic state has not been directly obtained in our perturbative calculation. Nevertheless, it is not difficult to obtain the $D_{s0}^*(2317)$ by using an iterated method (e.g., Schrödinger equation) with the strong attractive DK interaction potential. The iterated method can generate the bound state because the nonperturbative dynamics is considered. The detailed description of the $D_{s0}^*(2317)$ will also be given in the forthcoming works.

For the antikaon- D meson phase shifts, the $D\bar{K}(I=1)$ S wave and all P waves have repulsions. Apparently, the bound state or resonance cannot be found in these waves. Surprisingly, we obtain strong attractions in the both $D\bar{K}(I=0)$ and $D_s\bar{K}$ S waves. The first-order contribution almost cancels the second-order one in the $D\bar{K}(I=0)$ S wave, and the third-order contribution dominates this wave. However, the total contribution is still very large. The resulting strong attraction in this wave is consistent with the lattice QCD result, which indicates that there exists a virtual bound state in $D\bar{K}(I=0)$ S wave [66]. In the $D_s\bar{K}$ S wave, the attraction is obtained from each order. The total attraction is very strong and supports the existence of a bound state. This wave corresponds to the possible $D_0^*(2400)$ signal based on the coupled-channel analysis of the $D\pi$, $D\eta$ and $D_s\bar{K}$ scattering amplitudes in ref. [86]. This is also consistent with the strong attraction in the $D\pi(I=1/2)$ S wave.

For the eta- D meson phase shifts, there are repulsions in all P wave and strong attractions in

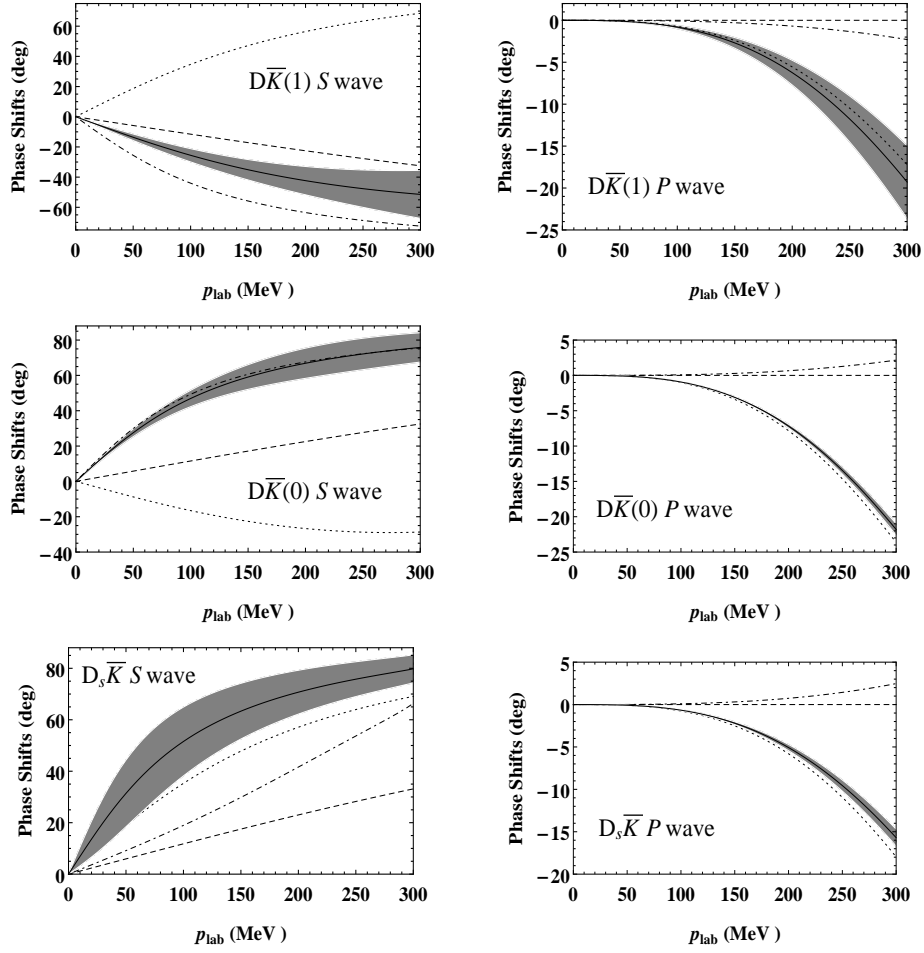


Figure 5: Predictions for the antikaon- D meson phase shifts versus the antikaon laboratory momentum at physical meson values. The notation is the same as in Fig. 3.

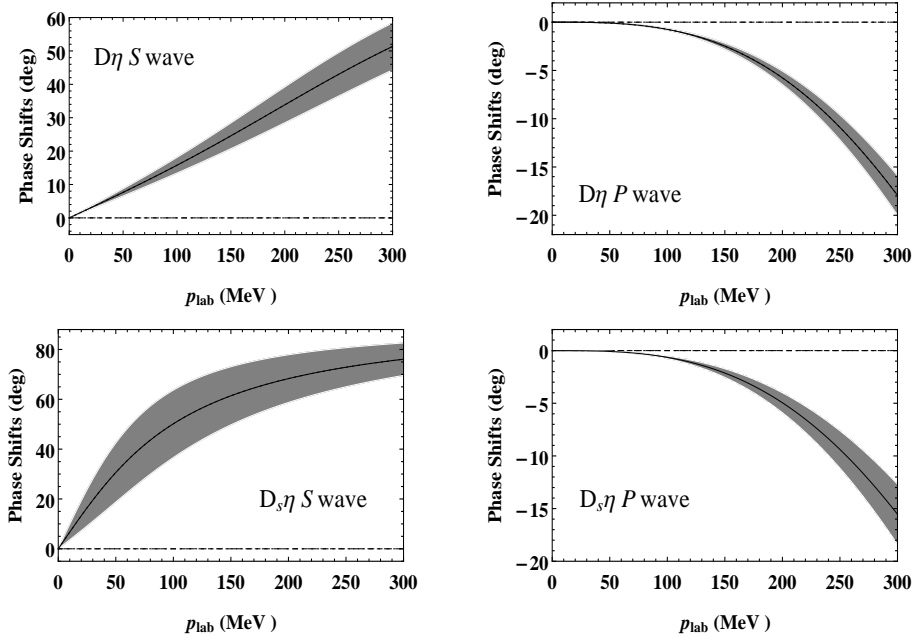


Figure 6: Predictions for the eta- D meson phase shifts versus the eta laboratory momentum. The notation is the same as in Fig. 3.

Table 2: Predictions of the scattering lengths for the light pseudoscalar meson and D meson at the physical meson values. The scattering lengths are in units of fm.

Sca. Len.	$\mathcal{O}(p)$	$\mathcal{O}(p^2)$	$\mathcal{O}(p^3)$	Total	Liu2013[63]	Guo2019[76]
$a_{(0,D\pi)}^{(3/2)}$	-0.24	0.23	-0.16	-0.17(6)	-0.100(2)	$-0.103_{-0.003}^{+0.003}$
$a_{(0,D\pi)}^{(1/2)}$	0.48	0.23	0.00	0.71(16)	$0.37_{-0.02}^{+0.03}$	$0.40_{-0.02}^{+0.03}$
$a_{(0,D_s\pi)}$	0.00	0.06	-0.08	-0.02(0)	-0.002(1)	$0.012_{-0.003}^{+0.003}$
$a_{(0,DK)}^{(1)}$	0.00	0.45	-0.24	0.21(1)	$0.07_{-0.03}^{+0.03} + i0.17_{-0.01}^{+0.02}$	$-0.01_{-0.03}^{+0.05} + i0.39_{-0.04}^{+0.04}$
$a_{(0,DK)}^{(0)}$	1.01	2.90	2.65	6.57(318)	$-0.84_{-0.22}^{+0.17}$	$-1.51_{-2.35}^{+0.72}$
$a_{(0,D_sK)}$	-0.51	1.69	-1.96	-0.78(19)	-0.18(1)	$-0.20_{-0.01}^{+0.01}$
$a_{(0,D\bar{K})}^{(1)}$	-0.51	1.67	-2.38	-1.21(19)	-0.20(1)	$-0.20_{-0.01}^{+0.01}$
$a_{(0,D\bar{K})}^{(0)}$	0.51	-0.78	2.86	2.58(19)	0.84(15)	21.9
$a_{(0,D_s\bar{K})}$	0.51	1.69	0.78	2.98(161)	$-0.09_{-0.05}^{+0.06} + i0.44_{-0.05}^{+0.05}$	$-0.57_{-0.04}^{+0.06} + i0.35_{-0.07}^{+0.08}$
$a_{(0,D\eta)}$	0.00	0.67	0.00	0.67(9)		$0.29_{-0.22}^{+0.15} + i0.61_{-0.26}^{+0.30}$
$a_{(0,D_s\eta)}$	0.00	2.97	0.00	2.97(139)		$-0.39_{-0.03}^{+0.05} + i0.06_{-0.02}^{+0.02}$

all S waves. The first- and third-order contributions are almost zero in both $D\eta$ and $D_s\eta$ S waves, since the tree amplitudes at the first- and third-order are zero, and the one-loop amplitudes at the third order are small. The $D\eta$ S wave also corresponds to the $D_0^*(2400)$ in the coupled-channel $D\pi$, $D\eta$ and $D_s\bar{K}$ scattering amplitudes [86]. It is interesting that the $D_s\eta$ S wave has also strong attractions and supports the existence of a bound state or resonance. This will be further studied in the future works.

From the phase shifts for the light pseudoscalar meson and heavy meson scattering, we can see that there are repulsions in all P waves, and the bound states or resonances cannot be dynamically generated in these waves. However, we find that the phase shifts in the $D\pi(I = 1/2)$, $DK(I = 0)$, $D\bar{K}(I = 0)$, $D_s\bar{K}$, $D\eta$ and $D_s\eta$ S waves are so strong that the bound states or resonances may be generated dynamically in these channels.

5.3 Scattering lengths and scattering volumes

Finally, we calculate the scattering lengths for the S waves and the scattering volumes for the P waves with Eq. (47) at the physical meson values. The scattering lengths are shown in Table 2, and the scattering volumes are shown in Table 3. The scattering lengths and the scattering volumes are obtained by using an incident light meson momentum $p_{\text{lab}} = 10$ MeV to approximate its value at threshold. The errors of the scattering lengths and the scattering volumes in our calculations are estimated from the statistical errors of the LECs using the error propagation formula with the correlations. Similarly, the errors at the different orders are not given, although we present the values of the scattering lengths and the scattering volumes from the different orders. A good convergence is not achieved for the scattering lengths, while a good convergence is obtained for the scattering volumes.

The scattering lengths in the channels $D\pi(I = 1/2)$, $DK(I = 0)$, $D\bar{K}(I = 0)$, $D_s\bar{K}$, $D\eta$ and $D_s\eta$ have large values. A bound state or resonance may be generated in these channels. The other scattering lengths are either small or negative, where a bound state or resonance cannot be dynamically generated. We obtain a large positive value for the channel $DK(I = 0)$ which corresponds to the $D_{s0}^*(2317)$. A channel with a bound state should have a large negative scattering length, as obtained from refs. [63, 76]. However, the correct scattering length for this channel was obtained in our previous works [70] through the iterated method.

We obtain the negative values for the scattering volumes in all channels. Therefore, a bound state or resonance cannot be generated in the P waves. The values from the first-order contributions are zero, and the values from the third-order contributions are small. Then the second order contributions dominate the total values. A good convergence is obtained for the scattering volumes at the third chiral order.

Table 3: Predictions of the scattering volumes for the light pseudoscalar meson and D meson at the physical meson values. The scattering volumes are in units of fm^3 . Note that, the values for the $\mathcal{O}(p)$ in all channels are zero, and are not shown.

Sca. Vol.	$\mathcal{O}(p^2)$	$\mathcal{O}(p^3)$	Total
$a_{(1,D\pi)}^{(3/2)}$	-0.33	-0.01	-0.34(6)
$a_{(1,D\pi)}^{(1/2)}$	-0.33	0.02	-0.31(4)
$a_{(1,D_s\pi)}$	-0.40	0.00	-0.40(4)
$a_{(1,DK)}^{(1)}$	-0.24	0.00	-0.24(2)
$a_{(1,DK)}^{(0)}$	-0.16	0.05	-0.11(0)
$a_{(1,D_sK)}$	-0.20	-0.02	-0.22(5)
$a_{(1,D\bar{K})}^{(1)}$	-0.20	-0.02	-0.22(5)
$a_{(1,D\bar{K})}^{(0)}$	-0.28	0.02	-0.26(1)
$a_{(1,D_s\bar{K})}$	-0.20	0.02	-0.18(1)
$a_{(1,D\eta)}$	-0.22	0.00	-0.22(3)
$a_{(1,D_s\eta)}$	-0.18	0.00	-0.18(3)

6 Summary

In summary, we have calculated the complete T matrices of the elastic light pseudoscalar meson and heavy meson scattering up to the third order in HMChPT. We fitted the phase shifts and the scattering lengths from lattice QCD at nonphysical meson values to determine the LECs. This led to a good description of the phase shifts below the pion/kaon momentum 200 MeV and the scattering lengths at the nonphysical meson values for the channels excluding a bound state or resonance. We also obtained the LEC uncertainties and their mutual correlations through the statistical regression analysis. We predicted the S - and P -wave phase shifts for the light pseudoscalar meson and heavy meson scattering using these LECs at the physical meson values. We found that the phase shifts in the $D\pi(I = 1/2)$, $DK(I = 0)$, $D\bar{K}(I = 0)$, $D_s\bar{K}$, $D\eta$ and $D_s\eta$ S waves are strong enough to generate a bound state or resonance. The channel $DK(I = 0)$ corresponds to the well-known $D_{s0}^*(2317)$. The coupled channels $D\pi(I = 1/2)$, $D_s\bar{K}$ and $D\eta$ may correspond to the $D_0^*(2400)$. The channels $D\bar{K}(I = 0)$ and $D_s\eta$ may generate the respective bound state or resonance. However, as expected, we cannot obtain directly a bound state or resonance in our perturbative calculations. This issue can be successfully solved by the nonperturbative method, and the calculations including the nonperturbative dynamics will be presented in the forthcoming works. The P wave phase shifts in all channels are repulsive, and the bound states or resonances cannot be dynamically generated in these waves. We also predicted the scattering lengths and the scattering volumes using the LECs at the physical meson values. The scattering lengths also have large values in the channels $D\pi(I = 1/2)$, $DK(I = 0)$, $D\bar{K}(I = 0)$, $D_s\bar{K}$, $D\eta$ and $D_s\eta$, which indicate that a bound state or resonance may be generated in these channels. However, the correct scattering lengths for these channels should be obtained through the iterated method. We obtained the negative values for the scattering volumes in all channels, and a bound state or resonance cannot be generated in the P waves. In addition, we obtained a good convergence for the scattering volumes at the third chiral order. In order to study the bound states or resonances directly, the calculation including the nonperturbative dynamics is necessary. We wish our present calculations may provide a possibility to investigate the heavy meson-heavy meson interaction in the HMChPT.

Acknowledgments

This work is supported by the National Natural Science Foundation of China under Grants No. 11975033, No. 12070131001 and No. 12147127, and China Postdoctoral Science Foundation (Grant No. 2021M700251).

References

- [1] S. Weinberg. Phenomenological Lagrangians. *Physica A*, 96:327–340, 1979.
- [2] S. Scherer and M. R. Schindler. A primer for chiral perturbation theory. *Lect. Notes Phys.*, 830:pp.1–338, 2012.
- [3] R. Machleidt and D. R. Entem. Chiral effective field theory and nuclear forces. *Phys. Rept.*, 503:1–75, 2011.
- [4] J. Gasser, M. E. Sainio, and A. Svarc. Nucleons with Chiral Loops. *Nucl. Phys. B*, 307:779–853, 1988.
- [5] E. E. Jenkins and A. V. Manohar. Baryon chiral perturbation theory using a heavy fermion Lagrangian. *Phys. Lett. B*, 255:558–562, 1991.
- [6] V. Bernard, N. Kaiser, J. Kambor, and U.-G. Meißner. Chiral structure of the nucleon. *Nucl. Phys. B*, 388:315–345, 1992.
- [7] C. Ordóñez and U. van Kolck. Chiral lagrangians and nuclear forces. *Phys. Lett. B*, 291:459–464, 1992.
- [8] E. Epelbaum, W. Glöckle, and U.-G. Meißner. Nuclear forces from chiral lagrangians using the method of unitary transformation (i): Formalism. *Nucl. Phys. A*, 637:107–134, 1998.
- [9] N. Fettes, U.-G. Meißner, and S. Steininger. Pion-nucleon scattering in chiral perturbation theory (I): Isospin symmetric case. *Nucl. Phys. A*, 640:199–234, 1998.
- [10] N. Kaiser, R. Brockmann, and W. Weise. Peripheral nucleon-nucleon phase shifts and chiral symmetry. *Nucl. Phys. A*, 625:758–788, 1997.
- [11] X.-W. Kang, J. Haidenbauer, and U.-G. Meißner. Antinucleon-nucleon interaction in chiral effective field theory. *JHEP*, 02:113, 2014.
- [12] D. R. Entem, N. Kaiser, R. Machleidt, and Y. Nosyk. Peripheral nucleon-nucleon scattering at fifth order of chiral perturbation theory. *Phys. Rev. C*, 91:014002, 2015.
- [13] N. Kaiser. Density-dependent NN interaction from subsubleading chiral 3N forces: Intermediate-range contributions. *Phys. Rev. C*, 101:014001, 2020.
- [14] N. Kaiser. Chiral corrections to kaon nucleon scattering lengths. *Phys. Rev. C*, 64:045204, 2001. [Erratum: *Phys. Rev. C* 73, 069902(2006)].
- [15] Y.-R. Liu and S.-L. Zhu. Meson-baryon scattering lengths in HB χ PT. *Phys. Rev. D*, 75:034003, 2007.
- [16] J. Haidenbauer, S. Petschauer, N. Kaiser, U.-G. Meißner, A. Nogga, and W. Weise. Hyperon-nucleon interaction at next-to-leading order in chiral effective field theory. *Nucl. Phys. A*, 915:24–58, 2013.
- [17] B.-L. Huang and Y.-D. Li. Kaon-nucleon scattering to one-loop order in heavy baryon chiral perturbation theory. *Phys. Rev. D*, 92:114033, 2015. [Erratum: *Phys. Rev. D* 95, 019903(2017)].
- [18] B.-L. Huang, J.-S. Zhang, Y.-D. Li, and N. Kaiser. Meson-baryon scattering to one-loop order in heavy baryon chiral perturbation theory. *Phys. Rev. D*, 96:016021, 2017.
- [19] B.-L. Huang and J. Ou-Yang. Pion-nucleon scattering to $\mathcal{O}(p^3)$ in heavy baryon SU(3) chiral perturbation theory. *Phys. Rev. D*, 101:056021, 2020.
- [20] B.-L. Huang. Pion-nucleon scattering to order p^4 in SU(3) heavy baryon chiral perturbation theory. *Phys. Rev. D*, 102:116001, 2020.
- [21] B.-L. Huang, J.-B. Cheng, and S.-L. Zhu. Peripheral nucleon-nucleon scattering at next-to-next-to-leading order in SU(3) heavy baryon chiral perturbation theory. *Phys. Rev. D*, 104:116030, 2021.
- [22] T. Becher and H. Leutwyler. Baryon chiral perturbation theory in manifestly Lorentz invariant form. *Eur. Phys. J. C*, 9:643–671, 1999.
- [23] J. Gegelia and G. Japaridze. Matching heavy particle approach to relativistic theory. *Phys. Rev. D*, 60:114038, 1999.
- [24] T. Fuchs, J. Gegelia, G. Japaridze, and S. Scherer. Renormalization of relativistic baryon chiral perturbation theory and power counting. *Phys. Rev. D*, 68:056005, 2003.
- [25] M. R. Schindler, T. Fuchs, J. Gegelia, and S. Scherer. Axial, induced pseudoscalar, and

- pion-nucleon form-factors in manifestly Lorentz-invariant chiral perturbation theory. *Phys. Rev. C*, 75:025202, 2007.
- [26] L. S. Geng, J. Martin Camalich, L. Alvarez-Ruso, and M. J. Vicente Vacas. Leading SU(3)-breaking corrections to the baryon magnetic moments in chiral perturbation theory. *Phys. Rev. Lett.*, 101:222002, 2008.
- [27] J. M. Alarcón, J. Martin Camalich, and J. A. Oller. The chiral representation of the πN scattering amplitude and the pion-nucleon sigma term. *Phys. Rev. D*, 85:051503, 2012.
- [28] X. L. Ren, L. S. Geng, J. Martin Camalich, J. Meng, and H. Toki. Octet baryon masses in next-to-next-to-next-to-leading order covariant baryon chiral perturbation theory. *JHEP*, 12:073, 2012.
- [29] Y.-H. Chen, D.-L. Yao, and H. Q. Zheng. Analyses of pion-nucleon elastic scattering amplitudes up to $\mathcal{O}(p^4)$ in extended-on-mass-shell subtraction scheme. *Phys. Rev. D*, 87:054019, 2013.
- [30] D.-L. Yao, D. Siemens, V. Bernard, E. Epelbaum, A. M. Gasparyan, J. Gegelia, H. Krebs, and U.-G. Meißner. Pion-nucleon scattering in covariant baryon chiral perturbation theory with explicit Delta resonances. *JHEP*, 05:038, 2016.
- [31] J.-X. Lu, C.-X. Wang, Y. Xiao, L.-S. Geng, J. Meng, and P. Ring. Accurate Relativistic Chiral Nucleon-Nucleon Interaction up to Next-to-Next-to-Leading Order. *Phys. Rev. Lett.*, 128:142002, 2022.
- [32] M. B. Wise. Chiral perturbation theory for hadrons containing a heavy quark. *Phys. Rev. D*, 45:R2188, 1992.
- [33] B. Wang, L. Meng, and S.-L. Zhu. Hidden-charm and hidden-bottom molecular pentaquarks in chiral effective field theory. *JHEP*, 11:108, 2019.
- [34] L. Meng, B. Wang, and S.-L. Zhu. $\Sigma_c N$ interaction in chiral effective field theory. *Phys. Rev. C*, 101:064002, 2020.
- [35] B. Wang, L. Meng, and S.-L. Zhu. $D^{(*)}N$ interaction and the structure of $\Sigma_c(2800)$ and $\Lambda_c(2940)$ in chiral effective field theory. *Phys. Rev. D*, 101:094035, 2020.
- [36] K. Chen, B.-L. Huang, B. Wang, and S.-L. Zhu. $\Sigma_c \Sigma_c$ interactions in chiral effective field theory. arXiv: 2204.13316.
- [37] L. Meng, B. Wang, G.-J. Wang, and S.-L. Zhu. Chiral perturbation theory for heavy hadrons and chiral effective field theory for heavy hadronic molecules. arXiv: 2204.08716.
- [38] B. Aubert et al. Observation of a narrow meson decaying to $D_s^+ \pi^0$ at a mass of 2.32-GeV/ c^2 . *Phys. Rev. Lett.*, 90:242001, 2003.
- [39] P. Krokovny et al. Observation of the $D_{sJ}(2317)$ and $D_{sJ}(2457)$ in B Decays. *Phys. Rev. Lett.*, 91:262002, 2003.
- [40] D. Besson et al. Observation of a narrow resonance of mass 2.46 GeV/ c^2 decaying to $D_s^{*+} \pi^0$ and confirmation of the $D_{sJ}^*(2317)$ state. *Phys. Rev. D*, 68:032002, 2003. [Erratum: *Phys.Rev.D* 75, 119908 (2007)].
- [41] S. K. Choi et al. Observation of a narrow charmonium-like state in exclusive $B^\pm \rightarrow K^\pm \pi^+ \pi^- J/\psi$ decays. *Phys. Rev. Lett.*, 91:262001, 2003.
- [42] X. Liu. An overview of XYZ new particles. *Chin. Sci. Bull.*, 59:3815–3830, 2014.
- [43] J.-J. Xie, W.-H. Liang, and E. Oset. Hidden charm pentaquark and $\Lambda(1405)$ in the $\Lambda_b^0 \rightarrow \eta_c K^- p(\pi\Sigma)$ reaction. *Phys. Lett. B*, 777:447–452, 2018.
- [44] Y.-L. Ma and M. Harada. Chiral partner structure of doubly heavy baryons with heavy quark spin-flavor symmetry. *J. Phys. G*, 45:075006, 2018.
- [45] Y.-R. Liu, H.-X. Chen, W. Chen, X. Liu, and S.-L. Zhu. Pentaquark and Tetraquark states. *Prog. Part. Nucl. Phys.*, 107:237–320, 2019.
- [46] W.-H. Liang, N. Ikeno, and E. Oset. $\Upsilon(nI)$ decay into $B^{(*)} \bar{B}^{(*)}$. *Phys. Lett. B*, 803:135340, 2020.
- [47] Y. Dong, P. Shen, F. Huang, and Z. Zhang. Selected strong decays of pentaquark State $P_c(4312)$ in a chiral constituent quark model. *Eur. Phys. J. C*, 80:341, 2020.
- [48] Q. Wu, D.-Y. Chen, W.-H. Qin, and G. Li. Production of Z_{cs} in B and B_s decay. arXiv: 2111.13347.
- [49] C. Deng and S.-L. Zhu. Tcc+ and its partners. *Phys. Rev. D*, 105:054015, 2022.
- [50] C.-R. Deng and S.-L. Zhu. Decoding the double heavy tetraquark state T_{cc}^+ . arXiv: 2204.11079.
- [51] J. He and X. Liu. The quasi-fission phenomenon of double charm T_{cc}^+ induced by nucleon. *Eur. Phys. J. C*, 82:387, 2022.
- [52] H.-X. Chen, W. Chen, X. Liu, Y.-R. Liu, and S.-L. Zhu. An updated review of the new

- hadron states. arXiv: 2204.02649.
- [53] Z.-H. Wang and G.-L. Wang. Two-Body Strong Decay of the $2P$ and $3P$ Charmonium states. arXiv: 2204.08236.
 - [54] L. R. Dai, R. Molina, and E. Oset. Looking for the exotic $X_0(2866)$ and its $J^P = 1^+$ partner in the $\bar{B}^0 \rightarrow D^{(*)+} K^- K^{(*)0}$ reactions. arXiv: 2202.11973.
 - [55] T. Barnes, F. E. Close, and H. J. Lipkin. Implications of a DK molecule at 2.32 GeV. *Phys. Rev. D*, 68:054006, 2003.
 - [56] F.-K. Guo, P.-N. Shen, H.-C. Chiang, R.-G. Ping, and B.-S. Zou. Dynamically generated 0^+ heavy mesons in a heavy chiral unitary approach. *Phys. Lett. B*, 641:278–285, 2006.
 - [57] F.-K. Guo, P.-N. Shen, and H.-C. Chiang. Dynamically generated 1^+ heavy mesons. *Phys. Lett. B*, 647:133–139, 2007.
 - [58] V. Dmitrašinović. $D_{s0}^+(2317)$ - $D_0(2308)$ mass difference as evidence for tetraquarks. *Phys. Rev. Lett.*, 94:162002, 2005.
 - [59] E. van Beveren and G. Rupp. Observed $D_s(2317)$ and tentative $d(2100 - -2300)$ as the charmed cousins of the light scalar nonet. *Phys. Rev. Lett.*, 91:012003, 2003.
 - [60] G. S. Bali. $D_{s1}^+(2317)$: what can the lattice say? *Phys. Rev. D*, 68:071501, 2003.
 - [61] J. M. Flynn and J. Nieves. Elastic s-wave $B\pi$, $D\pi$, DK and $K\pi$ scattering from lattice calculations of scalar form-factors in semileptonic decays. *Phys. Rev. D*, 75:074024, 2007.
 - [62] D. Mohler, C. B. Lang, L. Leskovec, S. Prelovsek, and R. M. Woloshyn. $D_{s0}^*(2317)$ meson and D-meson-kaon scattering from lattice QCD. *Phys. Rev. Lett.*, 111:222001, 2013.
 - [63] L. Liu, K. Orginos, F.-K. Guo, C. Hanhart, and U.-G. Meißner. Interactions of charmed mesons with light pseudoscalar mesons from lattice QCD and implications on the nature of the $D_{s0}^*(2317)$. *Phys. Rev. D*, 87:014508, 2013.
 - [64] C. Alexandrou, J. Berlin, J. Finkenrath, T. Leontiou, and M. Wagner. Tetraquark interpolating fields in a lattice QCD investigation of the $D_{s0}^*(2317)$ meson. *Phys. Rev. D*, 101:034502, 2020.
 - [65] Y. Tan and J. Ping. $D_{s0}^*(2317)$ and $D_{s1}(2460)$ in an unquenched quark model. arXiv: 2111.04677.
 - [66] G. K. C. Cheung, C. E. Thomas, D. J. Wilson, G. Moir, M. Peardon, and S. Ryan. DK $I = 0$, $D\bar{K}$ $I = 0, 1$ scattering and the $D_{s0}^*(2317)$ from lattice QCD. *JHEP*, 02:100, 2021.
 - [67] Z. Yang, G.-J. Wang, J.-J. Wu, M. Oka, and S.-L. Zhu. Novel Coupled Channel Framework Connecting the Quark Model and Lattice QCD for the Near-threshold Ds States. *Phys. Rev. Lett.*, 128:112001, 2022.
 - [68] H.-X. Chen, W. Chen, X. Liu, Y.-R. Liu, and S.-L. Zhu. A review of the open charm and open bottom systems. *Rept. Prog. Phys.*, 80:076201, 2017.
 - [69] Y.-R. Liu, X. Liu, and S.-L. Zhu. Light Pseudoscalar Meson and Heavy Meson Scattering Lengths. *Phys. Rev. D*, 79:094026, 2009.
 - [70] B.-L. Huang, Z.-Y. Lin, and S.-L. Zhu. Light pseudoscalar meson and heavy meson scattering lengths to $\mathcal{O}(p^4)$ in heavy meson chiral perturbation theory. *Phys. Rev. D*, 105:036016, 2022.
 - [71] F.-K. Guo, C. Hanhart, and U.-G. Meißner. Interactions between heavy mesons and Goldstone bosons from chiral dynamics. *Eur. Phys. J. A*, 40:171–179, 2009.
 - [72] L. S. Geng, N. Kaiser, J. Martin-Camalich, and W. Weise. Low-energy interactions of nambu-goldstone bosons with d mesons in covariant chiral perturbation theory. *Phys. Rev. D*, 82:054022, 2010.
 - [73] P. Wang and X. G. Wang. Publisher’s note: Study of 0^+ states with open charm in the unitarized heavy meson chiral approach [phys. rev. d 86, 014030 (2012)]. *Phys. Rev. D*, 86:039903, Aug 2012.
 - [74] M. Altenbuchinger, L.-S. Geng, and W. Weise. Scattering lengths of Nambu-Goldstone bosons off D mesons and dynamically generated heavy-light mesons. *Phys. Rev. D*, 89:014026, 2014.
 - [75] D.-L. Yao, M.-L. Du, F.-K. Guo, and U.-G. Meißner. One-loop analysis of the interactions between charmed mesons and Goldstone bosons. *JHEP*, 11:058, 2015.
 - [76] Z.-H. Guo, L. Liu, U.-G. Meißner, J. A. Oller, and A. Rusetsky. Towards a precise determination of the scattering amplitudes of the charmed and light-flavor pseudoscalar mesons. *Eur. Phys. J. C*, 79:13, 2019.
 - [77] B. Borasoy and U.-G. Meißner. Chiral expansion of baryon masses and sigma-terms. *Annals Phys.*, 254:192–232, 1997.
 - [78] J. Gasser and U.-G. Meißner. On the phase of epsilon-prime. *Phys. Lett. B*, 258:219–224, 1991.

- [79] T. E. O. Ericson and W. Weise. *Pions and nuclei*. Clarendon Press, Oxford, UK, 1988.
- [80] G. Moir, M. Peardon, S. Ryan, C. E. Thomas, and D. J. Wilson. Coupled-Channel $D\pi$, $D\eta$ and $D_s\bar{K}$ Scattering from Lattice QCD. *JHEP*, 10:011, 2016.
- [81] A. Walker-Loud et al. Light hadron spectroscopy using domain wall valence quarks on an asqtad sea. *Phys. Rev. D*, 79:054502, 2009.
- [82] J. Dobaczewski, W. Nazarewicz, and P.-G. Reinhard. Error estimates of theoretical models: a Guide. *J. Phys. G*, 41:074001, 2014.
- [83] Carlsson B. D. et al. Uncertainty analysis and order-by-order optimization of chiral nuclear interactions. *Phys. Rev. X*, 6:011019, 2016.
- [84] P. A. Zyla et al. Review of Particle Physics. *Prog.Theor.Exp.Phys.*, 2020:083C01, 2020.
- [85] E. B. Gregory, F.-K. Guo, C. Hanhart, S. Krieg, and T. Luu. Confirmation of the existence of an exotic state in the πD system. arXiv: 2106. 15391.
- [86] M. Albaladejo, P. Fernandez-Soler, F.-K. Guo, and J. Nieves. Two-pole structure of the $D_0^*(2400)$. *Phys. Lett. B*, 767:465–469, 2017.